Cellular-resolution connectomics: challenges of dense neural circuit reconstruction

Moritz Helmstaedter

Neuronal networks are high-dimensional graphs that are packed into three-dimensional nervous tissue at extremely high density. Comprehensively mapping these networks is therefore a major challenge. Although recent developments in volume electron microscopy imaging have made data acquisition feasible for circuits comprising a few hundreds to a few thousands of neurons, data analysis is massively lagging behind. The aim of this perspective is to summarize and quantify the challenges for data analysis in cellular-resolution connectomics and describe current solutions involving online crowdsourcing and machine-learning approaches.

Brains are unique not in the number of cells they comprise (about 85 billion neurons in the case of the human brain[1,2]) but in the extent of direct and specific communication between their cells via synaptic connections (each neuron has on the order of 1,000 synaptically coupled partner neurons). Mapping the resulting complex connectivity graph is the goal of connectomics. At the coarse level, inter-areal projections are tracked either noninvasively using variants of diffusion imaging in humans[3] (see Review[4] in this issue) or invasively using tracer injections combined with high-throughput imaging in mice (Mouse Brain Architecture Project[5] (http://brainarchitecture.org/) and Allen Brain Connectivity Atlas (http://connectivity.brain-map.org/) among other initiatives; see Review[6] in this issue). However, the mapping coverage achieved using these approaches is still not sufficient to resolve the complete set of neuronal networks contained in the tissue. One voxel of magnetic resonance imaging data with typical one-cubic-millimeter resolution, for example, contains millions of neuronal cell bodies and several kilometers of neuronal wires.

At the other end of the resolution spectrum, the aim of connectomics is to image and analyze neuronal circuits densely in sufficiently large volumes but at single-cell and single-neurite resolution. Neuroscience is very data-poor in this respect, contrary to the assumptions made by contemporary simulation initiatives (The Human Brain Project[7]; http://www.humanbrainproject.eu/), and it is not known whether there are cases in which the measurement of cellular-resolution connectivity graphs can in fact be replaced by simplified low-order statistical assumptions about neuronal wiring. To date, only a few neuronal circuits have been analyzed comprehensively—with the connectivity map of the entire nervous system of *Caenorhabditis elegans*, comprising 302 neurons[8,9], being the most notable and largest for decades.

Neuronal-circuit reconstruction is so difficult because of the small size of neuronal processes and the extremely high packing density of the neuropil (**Fig. 1a**; here the term neuropil is used to describe nervous tissue containing densely packed axons and dendrites, even if interspersed with cell bodies, glia cells and blood vessels). For more than a century, the analysis of neuronal circuitry was therefore focused on using very sparse labeling techniques that stained only every 10,000th to 100,000th neuron in a given volume (**Fig. 1a**).

Only recent advances in high-throughput electron microscopy have made possible the imaging of substantial volumes of neuronal tissue at high resolution, allowing the reconstruction of larger circuits at a much faster pace. The main challenge, however, is the analysis of imaging data, which is currently the limiting step by several orders of magnitude. Overcoming this gap in data analysis is therefore the main methodological focus of cellular-resolution connectomics.

Resolution requirements

The mapping of dense circuits requires the reconstruction of a large fraction of the neuronal wires in a given volume of nerve tissue (**Fig. 1a**). In most cases,

Structure of Neocortical Circuits Group, Max Planck Institute of Neurobiology, Munich-Martinsried, Germany. Correspondence should be addressed to M.H. (mhelmstaedter@neuro.mpg.de).

RECEIVED 11 FEBRUARY; ACCEPTED 15 APRIL; PUBLISHED ONLINE 30 MAY 2013; DOI:10.1038/NMETH.2476

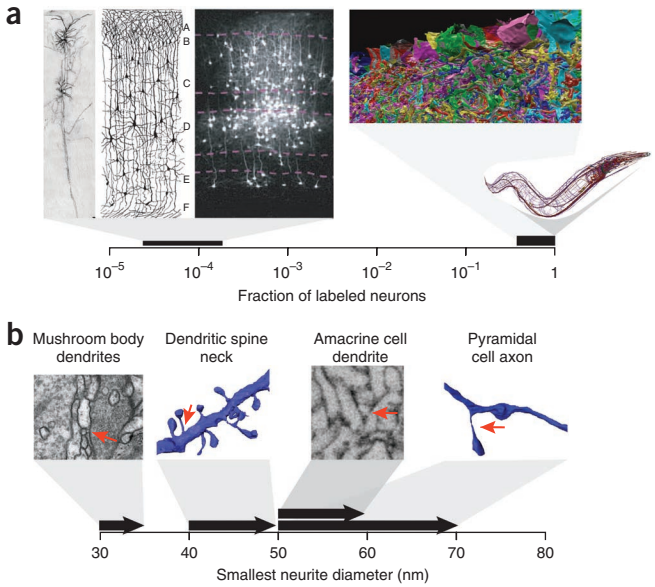

Figure 1 | Density of neuronal circuits and minimal resolution requirements. (**a**) Fraction of labeled neurons using light microscopy (left) and electron microscopy (right). In light microcopy images single neurons can be detected only because of extremely sparse staining. Images show (left to right): two synaptically coupled neurons from layers 4 and 2/3 in rat somatosensory cortex (modified from ref. 48), sketch of cortical neurons (from ref. 49, image from Wikimedia), population of fluorescently labeled neurons in neocortex that were presynaptic to one postsynaptic pyramidal neuron (modified from ref. 50), reconstruction of mouse retina inner plexiform layer (modified from ref. 36) and depiction of *C. elegans* neurons (from wormbase.org and openworm.org, courtesy of C. Grove and S. Larson). (**b**) Minimal resolution requirements for cellular connectomics. The thinnest structures in various neuronal circuits are indicated, from left to right: mushroom body dendrite (modified from ref. 12) dendrite of layer 4 neuron in mouse neocortex (image by B. Cowgill), starburst amacrine cell dendrite, modified from ref. 11, GABAergic axon in mouse neocortex (image by K. Boergens and N. Marahori). Not drawn to scale. Red arrows indicate examples of the respective neurites.

neuropil is largely isotropic: neuronal processes can locally turn in any direction, even in cases where there is a preferred direction such as the light axis in the retina or the radial developmental axis in the neocortex. This means that the lowest-resolution dimension of the imaging techniques used should account for the smallest neurite diameter in the chosen tissue volume. Examples of the smallest neurites in several parts of the nervous system (**Fig. 1b**) are dendritic spine necks (40–50 nanometer (nm) diameter, for example, in mouse hippocampus[10] and neocortex), the thinnest parts of mouse cortical axons (~50 nm; K.M. Boergens and M.H.; unpublished data), amacrine cell dendrites in the mouse retina (~50 nm (ref. 11; K.L. Briggman, personal communication) and dendrites in the fly mushroom body (~30 nm (ref. 12)). The minimal required imaging resolution is then roughly half the smallest neurite diameter, if one requires each neurite diameter to be represented by at least two voxels in the three-dimensional (3D) image data set. It may be possible in some cases to relieve this resolution requirement slightly based on prior knowledge about the shape of neurites and the continuity of intracellular organelles. Thus, the minimal required imaging resolution is ~20–30 nm for most circuits but can be as small as 10–15 nm in certain model systems.

Volume requirements: minimal circuit dimension

When mapping neuronal circuits (**Fig. 2a**), it is important to detect synaptic contacts between neurons, but it is in many cases even more important to be able to exclude synaptic connectivity between neurons to determine the structure of a wiring diagram (measuring the 'zeros' of the connectivity matrix). To exclude the existence of a synapse between two neurons, one has to image at least one of these two neurons in entirety. More precisely, in cases where neurons have an input part (for example, pyramidal cell dendrites, which are assumed to be only postsynaptic for chemical synapses) and an output part (for example, the axon of a local interneuron), at least one of the two neuronal arbors have to be fully contained in the imaged volume.

This notion implies that for each circuit to be mapped, one can define a minimal circuit volume that fulfills the criterion of sufficient completeness for a sufficient number of the relevant neurons (**Fig. 2b–e**). Then, the imaging technique should be capable of imaging volumes such that the smallest imaged dimension is at least as large as the minimal required circuit dimension.

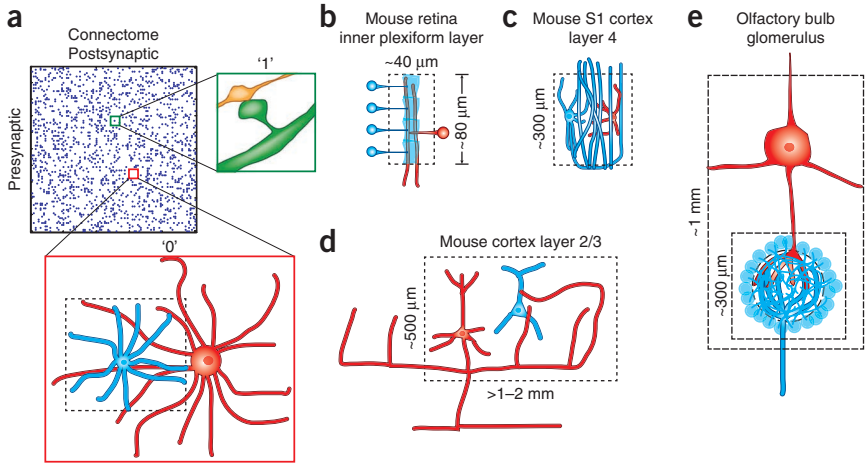

Figure 2 | Minimal circuit dimensions. (**a**) A 'connectome', the connectivity matrix between a set of presynaptic and postsynatptic neurons, with 15% positive entries ('1', blue dots) representing the existence of a synaptic connection between two neurons and 85% negative entries ('0', white) representing the absence of a synaptic connection. Detection of a synaptic connection is a local decision (on the order of a few micrometers; top right). To exclude synaptic connectivity between two neurons, at least one of them has to be imaged in its entirety, yielding the notion of a minimal circuit volume (dashed box) and the minimal circuit dimension (the smallest of the volumes' dimensions). (**b–e**) Approximate minimal circuit dimensions for several example circuits, based on the requirement to measure the existence and the absence of synaptic connections and the spatial extent of the relevant neurons in the circuit. Not drawn to scale. Dashed boxes indicate the respective minimal circuit volumes.

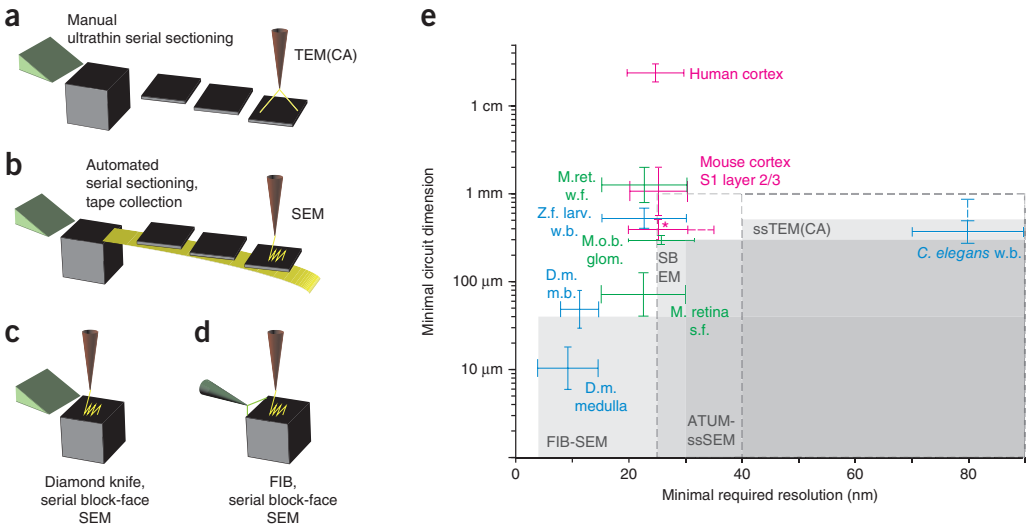

Figure 3 | Volume electron microscopy techniques for cellular connectomics and their spatial resolution and scope. (**a**–**d**) Sketches of the four most widely used methods for dense-circuit reconstruction: conventional manual ultrathin sectioning of neuropil (**a**) followed by TEM or TEMCA imaging[16] (**a**), ATUM-SEM[17] (**b**), SBEM[18] (**c**) and FIB-SEM[19] (**d**). In **a**,**b**, tissue is first sectioned and then (potentially later) transferred into the electron microscope for imaging. In **c**,**d**, the tissue block is abraded while imaging inside the electron microscope. (**e**) Approximate minimal resolution and smallest spatial dimension typically attainable with the imaging techniques in **a**–**d**, based on published results (gray shading); dashed lines indicate likely future extensions. Values also depend on the quality of staining and neurons of interest in a circuit. Approximate minimal resolution and minimal circuit dimension required to image indicated circuits. *C. elegans* w.b., *C. elegans* whole-brain reconstruction[8,9,35]; solid line indicates longest series from one worm and dashed line, the combined series length from three worms[9]. D.m. m.b., *Drosophila melanogaster* mushroom body; minimal required resolution based on estimate of smallest dendrites (30 nm diameter; **Fig. 1b**); D.m. medulla, *D. melanogaster* medulla, 1 cartridge (diameter of ~6 µm) with smallest processes less than 15 nm diameter. Human cortex, minimal circuit volume containing entire L5 pyramidal neuron dendrites and their local axons. Mouse cortex S1 layer 2/3, minimal circuit volume (**Fig. 2d**). *, mouse cortex S1 layer 4 minimal circuit volume (**Fig. 2c**). M.o.b.glom., mouse olfactory bulb, 1 glomerulus, only intraglomerular circuitry (**Fig. 2e**). M. retina s.f., mouse retina, small field (**Fig. 2b**). M.ret. w.f., mouse retina, wide field (including the largest amacrine and ganglion cells). Z.f. larv. w.b.: zebrafish larva whole brain.

For example, the minimal circuit volume for bipolar-to-ganglion cell connectivity in the mouse retina is dictated by the size of the axon of bipolar cells, which is contained in a volume of ~20 µm × 20 µm × 40 µm for most bipolar cells (20 µm in the plane of the retina, and 40 µm along the light axis; **Fig. 2b**). If one wants to map the circuits of roughly a dozen bipolar cells per bipolar cell type, the resulting minimal circuit volume is ~80 µm × 80 µm × 40 µm (**Fig. 2b**); thus the minimal circuit dimension is 40 µm. Other examples are the mouse olfactory bulb, where the entire circuit within one glomerulus, excluding mitral cells, is contained in a volume of ~300 µm × 300 µm × 300 µm (**Fig. 2e**). If one aims to include mitral cells into the circuit analysis, the minimal volume increases to ~1 mm × 500 µm × 500 µm (**Fig. 2e**; A. Schaefer; personal communication). In mouse neocortex, the minimal circuit volume is thought to be smallest in layer 4 of primary somatosensory cortex (~300 µm × 300 µm × 300 µm, **Fig. 2c**), it is ~1 mm × 1 mm × 500 µm in layer 2/3, ~3 mm × 3 mm × 1 mm in layer 5 and at least as large in other cortical areas where neurons have widespread axonal projections (**Fig. 2d**).

Together, the required minimal imaging resolution, as dictated by the smallest neurite diameters, and the minimal circuit dimension, as dictated by the types and spatial extent of the relevant neurons, differ widely between different circuit model systems. To map these circuits, it is therefore crucial to choose the appropriate volume imaging method (**Fig. 3**).

Volume electron microscopy techniques

All current imaging techniques used for cellular-resolution connectomics rely on sequential two-dimensional (2D) imaging of tissue combined with slicing, abrading or evaporating the tissue. Then images are combined into a 3D image volume. Only in this sense are today's imaging methods volume imaging methods.

The key techniques are serial-section transmission electron microscopy (ssTEM[9,13–15]) in some cases combined with fast camera arrays (TEMCA[16], **Fig. 3a**), automated serial-section tape-collection scanning electron microscopy (ATUM-SEM[17]; **Fig. 3b**), serial block-face SEM (SBEM[11,18], **Fig. 3c**) and focused ion beam SEM (FIB-SEM[19], **Fig. 3d**); these microscopy techniques are reviewed in ref. 20. Briefly, these methods differ in the sequence and quality of cutting and imaging, and provide different minimal imaging resolutions and dimensions. Essentially, the resolution is currently lowest, and the acquirable dimension is smallest, along the cutting axis.

In ssTEM (**Fig. 3a**), tissue is first cut into ultrathin sections, which are then imaged using TEM or speed-enhanced TEMCA. As sections are cut manually and are physically maintained for the imaging step, these techniques have a minimal resolution of ~40 nm. They provide large imaging areas in the plane of imaging but yield typically small dimensions along the cutting axis because manually cutting and maintaining more than a few thousand sections is hardly possible. ATUM-SEM (**Fig. 3b**) overcomes the cutting-thickness limitation of ssTEM by automated slicing and automated tape collection of the sections, yielding a minimal resolution of up to 30 nm and providing long series of collected sections. These are imaged using SEM as the collection tape is electron-dense. The two block-face techniques (**Fig. 3c**,**d**) interlace and invert the sequence of imaging and cutting: the entire tissue block is transferred into the electron microscope chamber, and

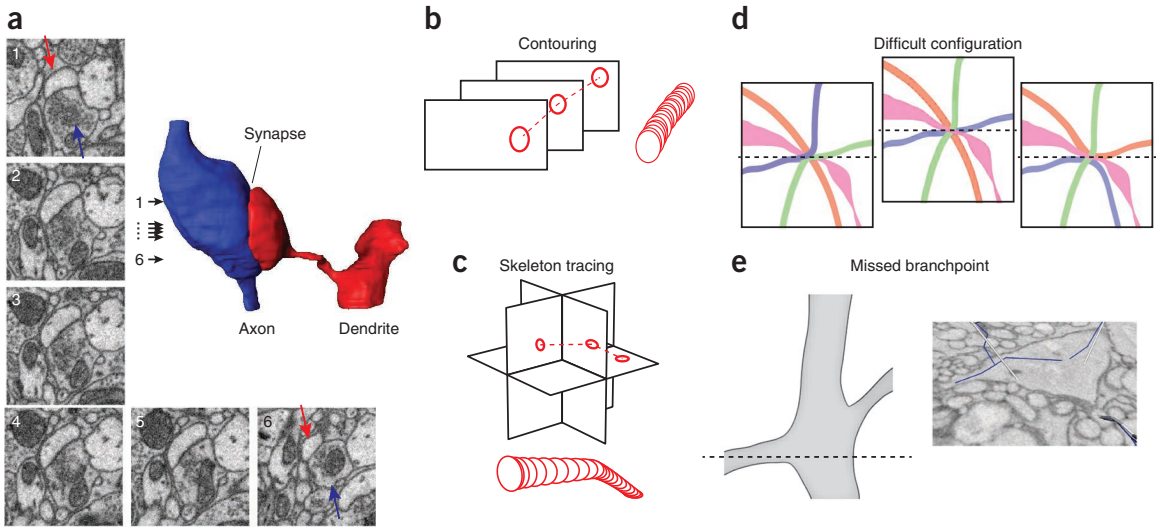

Figure 4 | Manual and automated reconstruction challenges in electron microscopy–based connectomics. (**a**) Volume reconstruction of a synaptic contact between an excitatory axon and dendritic spine in mouse somatosensory cortex imaged using SBEM (top right; K.M. Boergens and M.H., unpublished data). Images show electron microcopy slices at various depths; distance between slices 1 and 6 is 500 nm. (**b**,**c**) Manual data annotation is performed mostly either by contouring of neurite cross-sections (**b**) or center-line reconstruction (skeleton tracing, **c**). Contouring is ~50 times faster but provides no direct volume reconstruction. Modified from ref. 51. (**d**) Sketch of three possible neurite configurations for a configuration that automated algorithms typically cannot resolve but human annotators can (panels show three possible configurations). Dashed lines, imaging plane in which analysis is most difficult. Note that one neurite runs parallel to imaging plane (blue and green). Such a configuration is only resolvable if minimal resolution is greater than the smallest neurite diameter. Analysis may be facilitated when including priors about neurite diameters (pink neurite). (**e**) Branchpoint that can be missed by human annotators (unforced attention-related error[25]) corresponding to the dashed line in scheme on the left (from ref. 25; blue and white, skeletons traced independently by two expert annotators).

images are taken from the surface of the block using SEM. Then, the top of the tissue block is abraded either using a diamond-knife microtome installed into the electron microscope chamber (SBEM, **Fig. 3c**) or using a focused ion beam attached to the electron microscope (FIB-SEM, **Fig. 3d**). Diamond knife–based cutting currently limits the abrasion thickness to 25 nm but allows for long imaging sequences (smallest dimension is currently 300 µm (ref. 11), K.M. Boergens and M.H.; unpublished data), whereas FIB-SEM is unique in providing a minimal resolution of 4 nm, but so far limited in its smallest dimension (~40 µm (ref. 19)).

The relationship between the available electron microscopy imaging techniques and the resolution and size requirements of several example circuits is summarized in **Figure 3e**. In a nutshell, ssTEM is most amenable for circuits that can tolerate a minimal required resolution of more than 40 nm and a minimal circuit dimension of less than a few hundred micrometers, whereas FIB-SEM is uniquely suited for circuits that require very high imaging resolution, such as most circuits in the fly nervous system, but can tolerate smaller volumes. ATUM-SEM and SBEM are currently best suited for dense-circuit reconstruction in systems with ~25–30 nm minimal resolution and several hundred micrometers minimal circuit dimension. The aims of ongoing method developments are to increase the spatial scope along the cutting dimension, increase imaging speed in the plane of imaging and potentially decrease the cutting or abrasion thickness (**Fig. 3e**).

Circuit reconstruction

All high-resolution imaging techniques generate large volumes of images, which totaled several hundred gigabytes per data set for published projects[11,16,21], are currently around a dozen terabytes per data set and will likely be several petabytes per data set in the foreseeable future. To reconstruct neuronal circuits from the imaging data, synapses have to be identified, and the pre- and postsynaptic neurites contributing to each synapse have to be followed back to their respective cell bodies to attribute the synapse to the correct neuron. As soon as the imaging resolution and staining quality are sufficient for detecting postsynaptic densities and synaptic vesicles (which are ~40 nm in diameter and thus at the same scale as most minimal neurite diameters, see above), the detection of synapses becomes feasible. Synapse detection is more difficult in systems where one presynaptic site can have multiple postsynaptic partners (such as in the mammalian retina and the fly optical system), presynaptic vesicle pools are small and/or postsynaptic specializations are difficult to identify (for example, symmetrical synapses of inhibitory axons in the neocortex).

In all cases, volume imaging substantially improves the detection of synapses compared to the identification of synapses in two-dimensional images. For example, the 3D imaging of a synapse in mouse neocortex (**Fig. 4a**, at 25 nm slice thickness using SBEM, K.M. Boergens and M.H., unpublished data) substantially improves the reliability of synapse detection: judging the synapse from just one of the 2D images may be questionable, but the sequence of several 2D images of the same synaptic location relieves uncertainty of detection. Synapse detection is additionally improved by high-resolution 3D imaging as obtained using FIB-SEM[22] and can in these cases be automated[22,23]. Automated synapse-detection methods for SBEM and ssTEM data are likely to become available soon.

The main challenge for cellular connectomics, however, is not the detection of synapses but the reconstruction of neuronal wires (**Fig. 4b–e**). This immense difficulty has two main origins: first, neurites vary greatly in diameter and in local entanglement, generating a substantial frequency of locations at which the path of

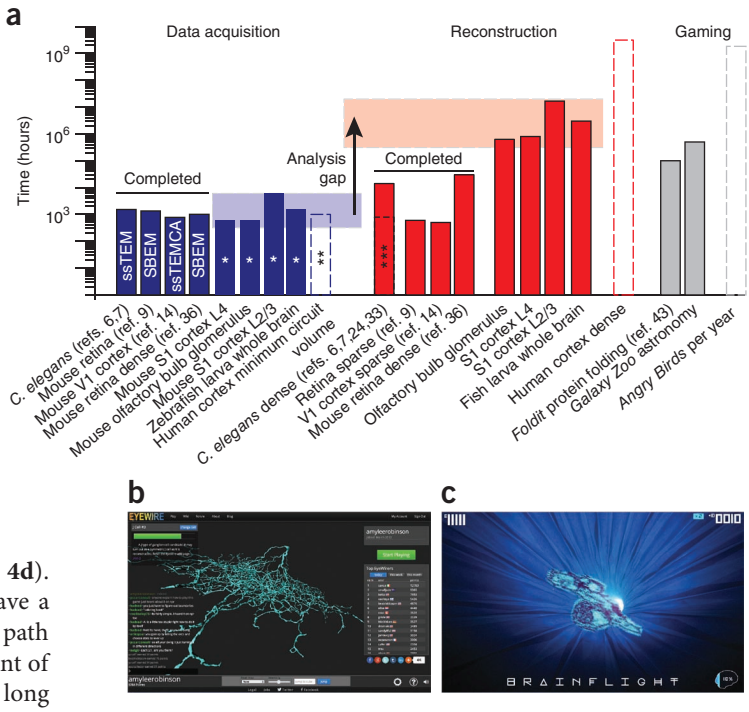

Figure 5 | Imaging and analysis times illustrating the analysis gap in cellular connectomics. (**a**) Data acquisition times and respective reconstruction durations for completed projects and estimates for ongoing or planned projects. Blue and red shading indicates experiment and reconstruction, respectively. Data-acquisition projections assume ~5 megahertz imaging speed and SBEM experiment (*); human cortex minimum circuit volume–acquisition projection assumes an additional ~200-fold increase in imaging speed as potentially attainable with multibeam electron microscopes (**). A recent *C. elegans* data analysis had a tenfold increase in the speed of annotation[26] (dashed line, ***). Gaming estimates are provided for successful science games in total annotation hours and an online casual game (*Angry Birds*) in annotation hours per year. *FoldIt* estimate is based on the number of players; *Galaxy Zoo* estimate is based on the reported number of classifications and an estimate of on average 30 seconds per classification. (**b**,**c**) Screen shots of ongoing online gaming initiatives in cellular connectomics: Eyewire (**b**; image courtesy of H.S. Seung) and Brainflight (**c**).

neurites can only be revealed after intense inspection (**Fig. 4d**). Second, and most notably, errors of neurite continuity have a highly correlated effect such that any neurite break along the path from a synapse to its soma creates an error in the assignment of the synapse to a neuron. As these entangled paths can be as long as several millimeters in many circuits (note that this is the neuronal path length between synapse and soma, not the Euclidean distance), neurite reconstruction has to be extremely reliable to provide tolerable error rates in the connectivity matrix.

In spite of these difficulties, human annotators can reconstruct electron microscopy data by either contouring the neurites in sequential image planes (**Fig. 4b** (refs. 21,24)) or by reconstructing only the neurite center line in three dimensions (**Fig. 4c** (refs. 25,26). Most notably, human annotators can resolve difficult locations with high accuracy (**Fig. 4d**). However, such annotation is very slow, and annotators make many unforced attention-related mistakes[25] (**Fig. 4e**).

In an attempt to speed up reconstruction, a main focus in connectomic data analysis was to devise automated reconstruction algorithms[15,22,27–33]. Unfortunately, however, these algorithms so far do not provide sufficient reconstruction accuracy to replace human annotators. Currently, automated reconstructions generate erroneous neurite breaks or erroneous neurite mergers every few tens of micrometers of neuronal path length, which results in the loss or misassignment of most of the synapses of a given neuron. Automated algorithms can, however, substantially support data annotation by human annotators, as discussed below.

Why do automated algorithms fail at resolving what human annotators can resolve? **Figure 4d** is an illustration of a local neurite configuration that could be interpreted in multiple ways by only subtle local changes of the membranes separating the respective neurites. Presently available automated algorithms are notoriously bad at resolving such locations, especially when the concerned neurites are very thin. It can be suspected that such neurite configurations can only be resolved when explicitly comparing the different possible segmentation solutions (**Fig. 4d**), which is what the human visual system may compute when inspecting such a location in the data. Recent developments in algorithms aim to account for such segmentation-based data analysis[31,34].

Analysis of electron microscopy data is thus meeting a substantial challenge: humans can solve difficult locations but are slow and make attention-based errors, whereas machines are efficient at solving easy locations but fail when neurites become small and their packing is dense.

The key approach to resolving the reconstruction problem in electron microscopy–based connectomics has therefore been to combine massive human data-annotation efforts with automated image analysis. In essence, human annotators provide the long-range connectivity information and solve the most difficult annotation problems, and automated algorithms provide the local volume reconstruction at less difficult locations. This analysis approach has been implemented in two variants: either automated algorithms are first used to presegment the imaging data, followed by manual inspection and correction (iterated proofreading[15,21,35], usually involving well-trained full-time annotators), or manual annotation is parallelized, followed by automated consensus computation, and by combination with local volume segmentation (forward-only annotation, usually using lightly trained part-time annotators such as undergraduate students[25]).

The analysis gap in cellular connectomics

What are the resulting experiment and analysis times for cellular-resolution connectomics today? In **Figure 5a**, durations for the accomplished circuit imaging and reconstruction experiments are reported as well as estimates for ongoing and envisioned projects.

Data acquisition took around several hundred to a thousand hours for the reconstruction of the *C. elegans* connectome[9] (ssTEM), the direction-selectivity circuit analysis in the mouse retina[11] (SBEM), a local circuit analysis experiment in V1 mouse cortex[16] (ssTEMCA) and the dense local reconstruction of the inner plexiform layer in mouse retina[36] (SBEM). This time was spread over several months for the ssTEM methods and compressed into 6–8 weeks in the SBEM experiments.

Imaging and acquisition speed has since substantially increased, bringing much larger volumes within the reach of a several-month continuous experiment: for example, one glomerulus in mouse

olfactory bulb (~300 μm × 300 μm × 300 μm), the minimal circuit volume in layer 4 of mouse S1 cortex (~300 μm × 300 μm × 300 μm) or the entire brain of the larva-stage zebra fish (~400 μm × 500 μm × 500 μm). Highly parallel SEM may promise an additional speed-up of more than two orders of magnitude, which would even enable the imaging of a relevant volume of human cortex (~2 cm × 2 cm × 1 cm). Improvements in imaging and acquisition rates appear to have moved many circuits of interest into the realm of experimental feasibility, which is ~1,000–2,000 hours of imaging time (**Fig. 5a**; continuous experiments of up to a year (~8,000 hours) may become feasible with improvements in automation).

However, if one considers the required reconstruction time, cellular-resolution connectomics imposes daunting challenges. The two recently published mouse connectomics studies made use of very sparse circuit reconstructions: only around 30 neurons were reconstructed for the direction-selectivity circuit analysis[11] and the V1 cortex study[16], already amounting to ~1,000 hours of analysis time.

For dense-circuit reconstruction, the *C. elegans* reconstruction took around 12 years of part-time work by one scientist[9,26], also amounting to around a few thousand hours of work. Including the additional studies[8,35], the *C. elegans* connectome may have consumed around 10,000–20,000 hours spread across three decades. The most recent mammalian dense-circuit reconstruction in mouse retina[36] took ~30,000 hours, by hundreds of part-time undergraduate annotators.

Thus, all cellular-resolution connectomics studies to date have involved thousands to tens-of-thousands of hours of reconstruction. Although imaging speed has substantially increased, reconstruction speed is massively lagging behind. For any of the proposed dense-circuit reconstructions (mouse neocortex, olfactory bulb, fish brain and human neocortex; **Fig. 5a**), analysis-time estimates are at least one if not several orders of magnitude larger than what has been accomplished to date (**Fig. 5a**): requirements for these envisioned projects are around several hundred thousand hours of manual labor per project. These enormous numbers constitute what can be called the analysis gap in cellular connectomics: although imaging larger circuits is becoming more and more feasible, reconstructing them is not.

Addressing the analysis problem

How is the field approaching this massive methodological challenge? There are two lines of solutions. First, improvements in automated algorithms promise to increase the efficiency of reconstruction by human annotators. Second, massive online crowd-sourcing initiatives are being built to 'recruit' the required work hours over the internet.

The current accuracy of automated classifiers is at least three orders of magnitude less than what is needed for reconstruction of entire neurons. It is therefore unlikely to expect that automated algorithms will soon take over image analysis for connectomics completely. Improvements in algorithms have saturated at the level of voxel classification ('voxel classifiers'[27,28,32,37–39]), and the current focus is on segmentation-based classifiers ('super-voxel classifiers'[31,34,40]). Rather than waiting for such algorithms to reach the required accuracy, automated methods have been made useful in reducing the analysis challenge when they were well integrated with human annotation[15,25,41–44]. For example, the estimates of circuit reconstruction reported in **Figure 5** are based on manual-algorithmic integration that already yielded a 10–50-fold increase in reconstruction efficiency.

Thus, on one hand, the key prospect for the improvement of automated analysis remains in lowering error rates (that is, generating longer correctly reconstructed neurite segments), but on the other hand, the focus is on better integration with human annotation. In an interesting twist, all automated methods rely heavily on training data. It is typically very expensive, however, to generate training data, and this in many cases limits algorithm improvements. Therefore, the attempts to recruit annotators to perform large amounts of human annotation, as described next, also may provide a critical boost to improve automated reconstruction methods.

Online crowd-sourcing has been successful in a few scientific fields: most notably the protein-folding game *FoldIt*[45] and the galaxy-classification initiative *Galaxy Zoo*[46]. Although these approaches proved very fruitful in their respective settings, the time requirements in cellular connectomics are still large by comparison. *Galaxy Zoo* has (over several years) probably recruited the work time required for the reconstruction of one dense cortical circuit (**Fig. 5a**). The comparison to casual gaming, however, seems promising: even a single successful game is reported to be played millions of hours every day, amounting to as many hours a year as would be needed to reconstruct a relevant piece of human cortex (~1 billion hours; **Fig. 5a**).

This setting of successful citizen-science games and the order of magnitude of hours spent online playing games has fueled hopes of recruiting the required analysis via the internet. As a first prerequisite, data annotation had to move online, overcoming the challenges of streaming the required data to clients' browsers. The Open Connectome project using the collaborative annotation toolkit for massive amounts of image data (CATMAID) software[47] focused on ssTEM and ssSEM data analysis, the Eyewire project for SBEM data (http://www.eyewire.org/; **Fig. 5b**) and the Brainflight project (http://www.brainflight.org/; **Fig. 5c**) are notable examples of online annotation, with Eyewire and Brainflight using game-like features to enhance engagement.

It is an exciting endeavor today to explore whether citizen science can help to overcome the massive analysis gap we are facing in cellular-resolution connectomics. Only if hundreds of thousands of hours can be recruited will dense-circuit reconstruction be feasible. It is also possible that improved automation will provide the crucial gain in the efficiency of analysis, but most likely it is going to be a combination of the two that will make dense-circuit reconstruction more and more realistic. Notably, it can be expected that once such large data sets are being reconstructed, the large amounts of training data needed to create more powerful analysis algorithms will be available. Then, finally, can connectomics analysis become a routine method with applications in many neuroscience laboratories, and cellular-resolution connectomics may further contribute to unraveling the computations neuronal circuits perform.

ACKNOWLEDGMENTS

I am grateful to the members of my laboratory for many fruitful discussions, specifically to K.M. Boergens, Y. Buckley, F. Isensee, N. Marahori, A. Mohn and H. Wissler for help with generating figures, and E. Dow for discussions concerning game development. I thank M. Berning, K.M. Boergens, E. Dow and A. Schaefer for helpful comments on the manuscript.

COMPETING FINANCIAL INTERESTS

The author declares no competing financial interests.

1. Herculano-Houzel, S. The human brain in numbers: a linearly scaled-up primate brain. *Front. Human Neurosci.* **3**, 31 (2009).
2. Azevedo, F.A. *et al.* Equal numbers of neuronal and nonneuronal cells make the human brain an isometrically scaled-up primate brain. *J. Comp. Neurol.* **513**, 532–541 (2009).
3. Wedeen, V.J. *et al.* The geometric structure of the brain fiber pathways. *Science* **335**, 1628–1634 (2012).
4. Craddock, R.C. Imaging human connectomes at the macroscale. *Nat. Methods* **10**, 524–539 (2013).
5. Bohland, J.W. *et al.* A proposal for a coordinated effort for the determination of brainwide neuroanatomical connectivity in model organisms at a mesoscopic scale. *PLOS Comput. Biol.* **5**, e1000334 (2009).
6. Osten, P. & Margrie, T.W. Mapping brain circuitry with a light microscope. *Nat. Methods* **10**, 515–523 (2013).
7. Markram, H. The blue brain project. *Nat. Rev. Neurosci.* **7**, 153–160 (2006).
8. Varshney, L.R., Chen, B.L., Paniagua, E., Hall, D.H. & Chklovskii, D.B. Structural properties of the *Caenorhabditis elegans* neuronal network. *PLOS Comput. Biol.* **7**, e1001066 (2011).
9. White, J.G., Southgate, E., Thomson, J.N. & Brenner, S. The structure of the nervous system of the nematode *Caenorhabditis elegans*. *Philos. Trans. R. Soc. Lond. B Biol. Sci.* **314**, 1–340 (1986).
10. Chicurel, M.E. & Harris, K.M. Three-dimensional analysis of the structure and composition of CA3 branched dendritic spines and their synaptic relationships with mossy fiber boutons in the rat hippocampus. *J. Comp. Neurol.* **325**, 169–182 (1992).
11. Briggman, K.L., Helmstaedter, M. & Denk, W. Wiring specificity in the direction-selectivity circuit of the retina. *Nature* **471**, 183–188 (2011).
12. Butcher, N.J., Friedrich, A.B., Lu, Z., Tanimoto, H. & Meinertzhagen, I.A. Different classes of input and output neurons reveal new features in microglomeruli of the adult *Drosophila* mushroom body calyx. *J. Comp. Neurol.* **520**, 2185–2201 (2012).
13. Fahrenbach, W.H. Anatomical circuitry of lateral inhibition in the eye of the horseshoe crab, *Limulus polyphemus*. *Proc. R. Soc. Lond. B Biol. Sci.* **225**, 219–249 (1985).
14. Harris, K.M. *et al.* Uniform serial sectioning for transmission electron microscopy. *J. Neurosci.* **26**, 12101–12103 (2006).
15. Mishchenko, Y. *et al.* Ultrastructural analysis of hippocampal neuropil from the connectomics perspective. *Neuron* **67**, 1009–1020 (2010).
16. Bock, D.D. *et al.* Network anatomy and *in vivo* physiology of visual cortical neurons. *Nature* **471**, 177–182 (2011).
17. Hayworth, K.J., Kasthuri, N., Schalek, R. & Lichtman, J.W. Automating the collection of ultrathin serial sections for large volume TEM reconstructions. *Microsc. Microanal.* **12** (suppl. 2), 86–87 (2006).
18. Denk, W. & Horstmann, H. Serial block-face scanning electron microscopy to reconstruct three-dimensional tissue nanostructure. *PLoS Biol.* **2**, e329 (2004).
19. Knott, G., Marchman, H., Wall, D. & Lich, B. Serial section scanning electron microscopy of adult brain tissue using focused ion beam milling. *J. Neurosci.* **28**, 2959–2964 (2008).
20. Briggman, K.L. & Bock, D.D. Volume electron microscopy for neuronal circuit reconstruction. *Curr. Opin. Neurobiol.* **22**, 154–161 (2012).
21. Cardona, A. *et al.* An integrated micro- and macroarchitectural analysis of the *Drosophila* brain by computer-assisted serial section electron microscopy. *PLoS Biol.* **8**, e1000502 (2010).
22. Kreshuk, A. *et al.* Automated detection and segmentation of synaptic contacts in nearly isotropic serial electron microscopy images. *PLoS ONE* **6**, e24899 (2011).
23. Becker, C., Ali, K., Knott, G. & Fua, P. Learning context cues for synapse segmentation in EM volumes. *Med. Image Comput. Comput. Assist. Interv.* **15**, 585–592 (2012).
24. Fiala, J.C. Reconstruct: a free editor for serial section microscopy. *J. Microsc.* **218**, 52–61 (2005).
25. Helmstaedter, M., Briggman, K.L. & Denk, W. High-accuracy neurite reconstruction for high-throughput neuroanatomy. *Nat. Neurosci.* **14**, 1081–1088 (2011).
Algorithm-based apparatus for combining the reconstructions of many slightly trained annotators into a consensus reconstruction, a prerequisite for large-scale crowd-sourcing.
26. Xu, M. *et al.* Computer assisted assembly of connectomes from electron micrographs: application to *Caenorhabditis elegans*. *PLoS ONE* **8**, e54050 (2013).
27. Jain, V. *et al.* Supervised learning of image restoration with convolutional networks. *IEEE 11th International Conference on Computer Vision* 1–8 (2007).
28. Jain, V., Seung, H.S. & Turaga, S.C. Machines that learn to segment images: a crucial technology for connectomics. *Curr. Opin. Neurobiol.* **20**, 653–666 (2010).
29. Turaga, S.C. *et al.* Convolutional networks can learn to generate affinity graphs for image segmentation. *Neural Comput.* **22**, 511–538 (2010).
30. Chklovskii, D.B., Vitaladevuni, S. & Scheffer, L.K. Semi-automated reconstruction of neural circuits using electron microscopy. *Curr. Opin. Neurobiol.* **20**, 667–675 (2010).
31. Andres, B. *et al.* 3D segmentation of SBFSEM images of neuropil by a graphical model over supervoxel boundaries. *Med. Image Anal.* **16**, 796–805 (2012).
32. Andres, B., Köthe, U., Helmstaedter, M., Denk, W. & Hamprecht, F. Segmentation of SBFSEM volume data of neural tissue by hierarchical classification. in *Pattern Recognition, Proc. DAGM 2008, Lecture Notes in Computer Science* (ed., G. Rigoll) **5096**, 142–152 (Springer, 2008).
33. Funke, J., Andres, B., Hamprecht, F.A., Cardona, A. & Cook, M. Efficient automatic 3D-reconstruction of branching neurons from EM data. *Proc. IEEE Conference on Computer Vision and Pattern Recognition* 1004–1011 (2012).
34. Jain, V. *et al.* Learning to agglomerate superpixel hierarchies. in *Advances in Neural Information Processing Systems* (eds., J. Shawe-Taylor, R.S. Zemel, P. Bartlett, F.C.N. Pereira and K.Q. Weinberger) **24**, 648–656 (2011).
35. Jarrell, T.A. *et al.* The connectome of a decision-making neural network. *Science* **337**, 437–444 (2012).
36. Helmstaedter, M., Briggman, K.L., Turaga, S., Jain, V., Seung, H.S. & Denk, W. Connectomic reconstruction of the inner plexiform layer in the mouse retina. *Nature* (in the press).
37. Turaga, S.C. *et al.* Convolutional networks can learn to generate affinity graphs for image segmentation. *Neural Comput.* **22**, 511–538 (2010).
38. Mishchenko, Y. Automation of 3D reconstruction of neural tissue from large volume of conventional serial section transmission electron micrographs. *J. Neurosci. Methods* **176**, 276–289 (2009).
39. Seyedhosseini, M. *et al.* Detection of neuron membranes in electron microscopy images using multi-scale context and radon-like features. *Med. Image Comput. Comput. Assist. Interv.* **14**, 670–677 (2011).
40. Vazquez-Reina, A. *et al.* Segmentation fusion for connectomics. *IEEE International Conference on Computer Vision* 177–184 (2011).
41. Sommer, C., Straehle, C., Koethe, U. & Hamprecht, F.A. ilastik: interactive learning and segmentation toolkit. *Proc. IEEE International Symposium on Biomedical Imaging* **8**, 230–233 (2011).
42. Straehle, C.N., Kothe, U., Knott, G. & Hamprecht, F.A. Carving: scalable interactive segmentation of neural volume electron microscopy images. *Med. Image Comput. Comput. Assist. Interv.* **14**, 653–660 (2011).
43. Jeong, W. *et al.* Ssecrett and NeuroTrace: interactive visualization and analysis tools for large-scale neuroscience data sets. *IEEE Comput. Graph. Appl.* **30**, 58–70 (2010).
44. Roberts, M. *et al.* Neural process reconstruction from sparse user scribbles. *Med. Image Comput. Comput. Assist. Interv.* **14**, 621–628 (2011).
45. Cooper, S. *et al.* Predicting protein structures with a multiplayer online game. *Nature* **466**, 756–760 (2010).
Example of a computer game used for scientific discovery.
46. Land, K. *et al.* Galaxy Zoo: the large-scale spin statistics of spiral galaxies in the Sloan Digital Sky Survey. *Mon. Not. R. Astron. Soc.* **388**, 1686–1692 (2008).
47. Saalfeld, S., Cardona, A., Hartenstein, V. & Tomancak, P. CATMAID: collaborative annotation toolkit for massive amounts of image data. *Bioinformatics* **25**, 1984–1986 (2009).
Online annotation platform for electron microscopy image data presented in successive 2D image planes.
48. Feldmeyer, D., Lubke, J., Silver, R.A. & Sakmann, B. Synaptic connections between layer 4 spiny neurone-layer 2/3 pyramidal cell pairs in juvenile rat barrel cortex: physiology and anatomy of interlaminar signalling within a cortical column. *J. Physiol. (Lond.)* **538**, 803–822 (2002).
49. Ramón y Cajal, S. *Textura del sistema nervioso del hombre y de los vertebrados* (Imprenta N. Moya, 1904).
50. Rancz, E.A. *et al.* Transfection via whole-cell recording *in vivo*: bridging single-cell physiology, genetics and connectomics. *Nat. Neurosci.* **14**, 527–532 (2011).
51. Helmstaedter, M. & Mitra, P.P. Computational methods and challenges for large-scale circuit mapping. *Curr. Opin. Neurobiol.* **22**, 162–169 (2012).